Accepted Manuscript

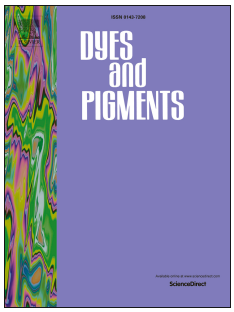

Charge Transfer NIR Dyes for Improved Photoacoustic Effect

An-Ping Xu, Hui-Hui Han, Jing Lu, Pei-Pei Yang, Yu-Juan Gao, Hong-Wei An, Di Zhang, Li-Zhong Li, Jing-Ping Zhang, Dong Wang, Lei Wang, Hao Wang

PII: S0143-7208(15)00430-1

DOI: 10.1016/j.dyepig.2015.11.003

Reference: DYPI 4994

To appear in: *Dyes and Pigments*

Received Date: 19 September 2015

Revised Date: 2 November 2015

Accepted Date: 4 November 2015

Please cite this article as: Xu A-P, Han H-H, Lu J, Yang P-P, Gao Y-J, An H-W, Zhang D, Li L-Z, Zhang J-P, Wang D, Wang L, Wang H, Charge Transfer NIR Dyes for Improved Photoacoustic Effect, *Dyes and Pigments* (2015), doi: 10.1016/j.dyepig.2015.11.003.

Graphical Abstract

A new class of NIR absorbing dyes accessed by a cycloaddition-cycloreversion reaction of alkynes with tetrafluoro-TCNQ is reported. Studies on the photoacoustic effect of the series of NIR dyes revealed a molar extinction coefficiency which contributed to the displayed photoacoustic effect.

Charge Transfer NIR Dyes for Improved Photoacoustic Effect

An-Ping Xu,‡[a,c] Hui-Hui Han,‡[b] Jing Lu,[d] Pei-Pei Yang,[a] Yu-Juan Gao,[a] Hong-Wei An,[a] Di Zhang,[a] Li-Zhong Li,[c] Jing-Ping Zhang,[d] Dong Wang,*[b] Lei Wang,*[a] and Hao Wang*[a]

[a]*CAS Key Laboratory for Biological Effects of Nanomaterials and Nanosafety, National Center for Nanoscience and Technology (NCNST)*
[b]*Beijing Key Laboratory of Function Materials for Molecule & Structure Construction, Department of Material Physics and Chemistry, School of Materials Science and Engineering, University of Science and Technology Beijing*
[c]*Key Laboratory of Catalysis and Materials Science of the State Ethnic Affairs Commission & Ministry of Education, South-Central University for Nationalities*
[d]*Faculty of Chemistry, Northeast Normal University Changchun,P. R. China*

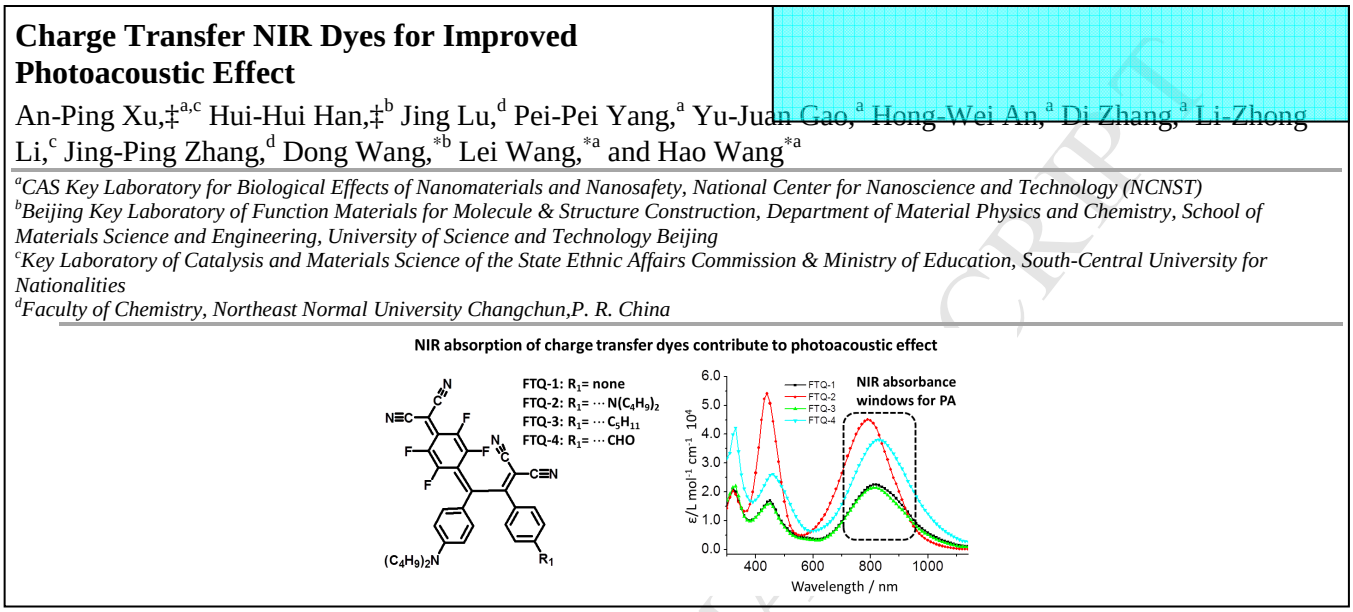

ELSEVIER

Dyes and Pigments

journal homepage: www.elsevier.com/locate/dyepig

Charge Transfer NIR Dyes for Improved Photoacoustic Effect

An-Ping Xu,‡[a,c] Hui-Hui Han,‡[b] Jing Lu,[d] Pei-Pei Yang,[a] Yu-Juan Gao,[a] Hong-Wei An,[a] Di Zhang,[a] Li-Zhong Li,[c] Jing-Ping Zhang,[d] Dong Wang,*[b] Lei Wang,*[a] and Hao Wang*[a]

[a]*CAS Key Laboratory for Biological Effects of Nanomaterials and Nanosafety, National Center for Nanoscience and Technology (NCNST)*

[b]*Beijing Key Laboratory of Function Materials for Molecule & Structure Construction, Department of Material Physics and Chemistry, School of Materials Science and Engineering, University of Science and Technology Beijing*

[c]*Key Laboratory of Catalysis and Materials Science of the State Ethnic Affairs Commission & Ministry of Education, South-Central University for Nationalities*

[d]*Faculty of Chemistry, Northeast Normal University Changchun,P. R. China*

ARTICLE INFO

Article history:

Received

Received in revised form

Accepted

Available online

Keywords:

Near-infrared

Dye

Photoacoustic effect

Bioimaging

Charge transfer

ABSTRACT

A new class of NIR absorbing dyes accessed by a cycloaddition-cycloreversion reaction of alkynes with 2,3,5,6-tetrafluoro-7,7,8,8-tetracyanoquinodimethane is reported. The photoacoustic effect of the new NIR dyes was systematically studied. The results validated the positive correlation between the molar extinction coefficient and the photoacoustic effect. All of the new NIR dyes showed higher photoacoustic intensities compared to indocyanine green dye, which is the standard organic dye widely used as a photoacoustic contrast agent. Finally, the nano-sized liposomes loaded with the NIR dye showed good stabilities and high photoacoustic intensities, and were utilized to image the cells in agarose gels for a long time. The study guides the future design of NIR dyes for photoacoustic molecular materials with high intensities and displays promising applications in biomedical photoacoustic imaging.

‡ These authors contributed equally to this work.

* Corresponding authors. Tel./fax: +86 82545759. E-mail addresses: wanghao@nanoctr.cn, (H. Wang), wanglei@nanoctr.cn (L. Wang) wangdong@ustb.edu.cn (D. Wang).

Introduction

The photoacoustic (PA) effect was discovered by Alexander Graham Bell in 1880.[1,2] The PA effect refers to the phenomenon wherein matter absorbs a short-pulsed laser beam and converts its energy into sound (*via* heat, which induces localized pressure changes). [3] Based on the PA effect, photoacoustic imaging (PAI) has been developed as a highly promising tool for studying intracellular physiological processes. PAI combines the high spatial resolution of ultrasonic imaging and the high contrast of optical imaging.[4,5] Both the set-up of PAI devices and PA contrast agents contribute to the imaging performance. Organic dyes with a maximum absorption in the NIR range, such as cyanine, [6] porphyrin[7] and borondipyrromethene derivatives, [8] are widely used PA contrast agents. The development of new PA molecular materials are limited because the influence of factors on the PA effect have seldom been systematically studied, resulting in a lack of guidance for the design of molecular PA contrast agents. [9-11] Recently, we focused on [2+2] cycloaddition-cycloreversion chemistry, between either tetracyanoethene (TCNE), 7,7,8,8-tetracyanoquinodimethane (TCNQ) or 2,3,5,6-tetrafluoro-7,7,8,8-tetracyanoquinodimethane (F_4-TCNQ) and 'electronically confused' alkynes. [12-14] The resulting adducts, especially those formed from F_4-TCNQ, had good solubility and were easily prepared in high yields. Notably, these adducts showed a strong absorption in the 700-900 nm region, which made them highly suitable contrast agents for PAI. Here we report a new series of NIR dyes (abbreviated as **FTQ**) based on F_4-TCNQ. The series of **FTQ** dyes was synthesized by a cycloaddition-cycloreversion reaction between F_4-TCNQ and *N*,*N*-dibutyl-4-ethynylanilines (having different substitutions for fine modulation of optical properties). The PA effect of the series of **FTQ** dyes was characterized and they exhibited a higher PA intensity than that of indocyanine green (ICG) under the same experimental conditions. **FTQ-4** was successfully utilized for long-term cell imaging when self-assembled into hydrophobic phospholipid bilayers of liposomes. To further understand PA molecular materials, the relationship between molecular structures and PA intensities was investigated. The results indicate that substitution with other electron-donating or electron-withdrawing groups can enhance the molar extinction coefficient and PA intensity, which is in agreement with photothermal theory. This work provides high performance PA molecular materials and can direct the design of new NIR absorbing dyes for PAI.

2. Experimental

2.1. Materials and methods

Reagents were purchased from commercial sources (Aldrich) and used without further purification. ^{1}H NMR spectra were measured on a Bruker AV500 NMR spectrometer (500 MHz) at 20 °C. Chemical shifts are reported in ppm downfield from $SiMe_4$, using the solvent's residual signal as an internal reference. FT-IR was recorded on a PerkinElmer LR-64912C Fourier transform infrared spectrophotometer. All MALDI-TOF-MS spectra were measured on a Shimadzu AXIMA-CFR mass spectrometer. The operation was performed at an accelerating potential of 20 kV by a linear positive ion mode with dithranol as a matrix. UV/Vis/NIR spectra were recorded in a quartz cuvette on a JASCO V-570 spectrophotometer. Elemental analyses were measured on a FLASH EA 1112 elemental analyzer. The reacting aromatic alkyne molecules are shown in **Scheme 1**. $\mathbf{a_1}$-$\mathbf{a_4}$, $\mathbf{b_4}$ and **FTQ-4** were synthesized according to literature methods.[13,14] The other photoacoustic effect molecules were synthesized and fully characterized by NMR, FT-IR, MS spectra and elemental analysis from which the chemical structures were verified.

*2.2.1. Synthesis of N,N-dibutyl-4-(phenylethynyl)aniline (**b_1**).* Monomer **a_4** (137 mg, 0.600 mmol) and bromobenzene (0.079 g, 0.500 mmol) were dissolved in TEA (150 mL) and THF (150 mL). After the solution was flushed with bubbling Ar gas for 30 min, $Pd(PPh_3)_2Cl_2$ (12.6 mg, 0.018 mmol) and CuI (5.7 mg, 0.030 mmol) were added. The reaction mixture was then stirred at 80 °C for 10 h under Ar atmosphere. The resulting mixture was concentrated, diluted with CH_2Cl_2, and filtered through a plug of silica gel. The solvent was removed under vacuum and the product was purified by column chromatography (SiO_2, petroleum ether/CH_2Cl_2=4:1) to give **b_1** (0.115 g, 63%) as a yellow oil liquid. ^{1}H NMR ($CDCl_3$, 500 MHz): δ = 1.00 (t, J=7.5 Hz, 6H), 1.43 (m, 4H), 1.63 (m, 4H), 3.33 (t, J=7.5 Hz, 4H), 6.61 (d, J=5.4 Hz, 2H), 7.31 (t, J=7.0 Hz, 1H), 7.36(t, J=7.0 Hz, 2H), 7.40 (d, J=5.1 Hz, 2H), 7.53 (d, J=7.5 Hz, 2H) ppm. FT-IR (KBr): υ=2947, 2850, 2200, 1587, 1515, 1379, 1160, 926, 804, 523 cm^{-1}. MALDI-TOF-MS (dithranol): m/z: calc'd for $C_{22}H_{27}N$: 305.21 g/mol, found: 306.3 g/mol $[MH]^+$. Elemental analysis calc'd (%) for $C_{22}H_{27}N$ (305.21): C 86.51, H 8.91, N 4.58; found: C 86.50, H 8.92, N 4.59.

*2.2.2. Synthesis of 2-(2-(4-(Dibutylamino)phenyl)-2-(4-(dicyanomethylene)-2,3,5,6-tetrafluorocyclohexa-2,5-dien-1-ylidene)-1-phenylethylidene)malononitrile (**FTQ-1**).* The monomer **b_5** (0.100 g, 0.328 mmol) and F_4-TCNQ (0.090 mg, 0.330 mmol) were dissolved in chlorobenzene (2 mL). The reaction mixture was then stirred at 100 °C for 2 h under Ar atmosphere. The solvent was removed under vacuum and the product was purified by column chromatography (SiO_2, CH_2Cl_2) to give **FTQ-1** (0.183 g, 96%) as a black red solid. ^{1}H NMR ($CDCl_3$, 500 MHz): δ = 1.06 (t, J=7.5 Hz, 6H), 1.50 (m, 4H), 1.78 (m, 4H), 3.62 (t, J=6.0 Hz, 4H), 6.87 (d, J=9.5 Hz, 2H), 7.39 (d, J=9.0 Hz, 2H), 7.54 (t, J=7.5 Hz, 2H), 7.63 (t, J=8.0 Hz, 3H) ppm. FT-IR (KBr): υ=2946, 2850, 2200, 1587, 1515, 1379, 1160, 922, 804, 529 cm^{-1}. MALDI-TOF-MS (dithranol): m/z: calc'd for $C_{34}H_{27}F_4N_5$: 581.22 g/mol, found: 582.3 g/mol $[MH]^+$. Elemental analysis calc'd (%) for $C_{34}H_{27}F_4N_5$ (581.22): C 70.21, H 4.68, N 12.04; found: C 70.20, H 4.68, N 12.05.

*2.2.3. Synthesis of 4,4'-(Ethyne-1,2-diyl)bis(N,N-dibutylaniline) (**b_2**).* **a_2** (0.166 g, 0.500 mmol) and **a_4** (0.137 g, 0.600 mmol) were dissolved in TEA (150 mL) and THF (150 mL). The $Pd(PPh_3)_2Cl_2$ (12.6 mg, 0.0180 mmol) and CuI (5.7 mg, 0.030 mmol) were added into the solution after bubbling with Ar gas for 30 min. The reaction mixture was then stirred at 40 °C for 10 h under an Ar atmosphere. The resulting mixture was concentrated, diluted with CH_2Cl_2, and filtered through a plug of silica gel. The solvent was removed under vacuum and the product was purified by column chromatography (SiO_2, petroleum ether/CH_2Cl_2=4:1) to give **b_1** (0.155 g, 78%) as a colorless solid. ^{1}H NMR ($CDCl_3$, 500 MHz): δ = 0.99 (t, J=7.5 Hz, 12H), 1.38 (m, 8H), 1.62 (m, 8H), 3.31 (t, J=7.5 Hz, 8H), 6.59 (d, J=8.5 Hz, 4H), 7.36 (d, J=8.5 Hz, 4H) ppm. FT-IR (KBr): υ=2947, 2874, 2200, 1587, 1527, 1441, 1367, 1024, 914, 804, 621, 523 cm^{-1}. MALDI-TOF-MS (dithranol): m/z: calc'd for $C_{30}H_{44}N_2$: 432.35 g/mol, found: 433.3 g/mol $[MH]^+$. Elemental analysis calc'd (%) for $C_{30}H_{44}N_2$ (432.69): C 83.28, H 10.25, N 6.47; found: C 83.27, H 10.26, N 6.47.

*2.2.4. Synthesis of 2-(2-(4-(Dibutylamino)phenyl)-2-(4-(dicyanomethylene)-2,3,5,6-tetrafluorocyclohexa-2,5-dien-1-ylidene)-1-(4-nitrophenyl)ethylidene)malononitrile (**FTQ-2**).* The monomer **b_1** (120 mg, 0.361 mmol) and F_4-TCNQ (0.090 g, 0.360 mmol) were dissolved in chlorobenzene (2 mL). After, the reaction mixture was then stirred at 100 °C for 2 h under Ar atmosphere. The solvent was removed under vacuum and the product was purified by column chromatography (SiO_2, CH_2Cl_2) to give **FTQ-2** (0.213 g, 97%) as a

black red solid. ^{1}H NMR ($CDCl_3$, 500 MHz): δ = 0.94 (t, J=7.5 Hz, 6H), 1.00 (t, J=7.5 Hz, 6H), 1.44 (m, 4H), 1.51 (m, 4H), 1.66 (m, 4H), 1.78 (m, 4H), 3.57 (t, J=7.0 Hz, 4H), 3.61 (t, J=7.0 Hz, 4H), 6.62 (d, J=9.0 Hz, 2H), 6.83 (d, J=9.5 Hz, 2H), 7.41 (d, J=9.0 Hz, 2H), 7.56 (d, J=9.0 Hz, 2H) ppm. FT-IR (KBr): υ=2947, 2874, 2187, 1587, 1527, 1441, 1367, 1024, 914, 804, 621, 523 cm^{-1}. MALDI-TOF-MS (dithranol): m/z: calc'd for $C_{42}H_{44}N_6F_4$: 708.84 g/mol, found: 709.6 g/mol $[MH]^+$. Elemental analysis calc'd (%) for $C_{42}H_{44}N_6F_4$ (708.84): C 71.17, H 6.26, N 11.86; found: C 71.19, H 6.28, N 11.87.

*2.2.5. Synthesis of N,N-dibutyl-4-((4-pentylphenyl)ethynyl)aniline (**b$_3$**).* **a$_4$** (0.137 g, 0.600 mmol) and 1-bromo-4-pentylbenzene (0.113 g, 0.500 mmol) were dissolved in TEA (150 mL) and THF (150 mL). The solution was flushed with bubbling Ar gas for 30 min. Then the $Pd(PPh_3)_2Cl_2$ (12.6 mg, 0.0180 mmol) and CuI (5.7 mg, 0.030 mmol) were added. The reaction mixture was then stirred at 80 °C for 10 h under Ar atmosphere. The resulting mixture was concentrated, diluted with CH_2Cl_2, and filtered through a plug of silica gel. The solvent was removed under vacuum and the product was purified by column chromatography (SiO_2, petroleum ether/CH_2Cl_2=7:1) to give **b$_3$** (0.135 mg, 60%) as a yellow oil liquid. ^{1}H NMR ($CDCl_3$, 500 MHz): δ = 0.94 (t, J=6.0 Hz, 3H), 1.00 (t, J=7.0 Hz, 6H), 1.39 (m, 8H), 1.68 (m, 6H), 2.65 (t, J=7.5 Hz, 2H), 3.33 (t, J=7.5 Hz, 4H), 6.62 (d, J=9.0 Hz, 2H), 7.17 (d, J=7.5 Hz, 2H), 7.40 (d, J=9.0 Hz, 2H), 7.45 (d, J=7.5 Hz, 2H) ppm. FT-IR (KBr): υ=2935, 2850, 2200, 1601, 1503, 1367, 1184, 112, 792, 731, 535 cm^{-1}. MALDI-TOF-MS (dithranol): m/z: calc'd for $C_{27}H_{37}N$: 375.29 g/mol, found: 376.2 g/mol $[MH]^+$. Elemental analysis calc'd (%) for $C_{27}H_{37}N$ (375.29): C 86.34, H 9.93, N 3.73; found: C 86.35, H 9.94, N 3.74.

*2.2.6. Synthesis of 2-(2-(4-(Dibutylamino)phenyl)-2-(4-(dicyanomethylene)-2,3,5,6-tetrafluorocyclohexa-2,5-dien-1-ylidene)-1-(4-pentylphenyl)ethylidene)malononitrile (**FTQ-3**).* The monomer **b$_2$** (112 mg, 0.300 mmol) and F_4-TCNQ (0.082 g, 0.30 mmol) were dissolved in chlorobenzene (2 mL). The reaction mixture was then stirred at 100 °C for 2 h under Ar atmosphere. The solvent was removed under vacuum and the product was purified by column chromatography (SiO_2, CH_2Cl_2) to give **FTQ-3** (0.19 g, 98%) as a black red solid. ^{1}H NMR ($CDCl_3$, 500 MHz): δ = 0.92 (t, J=6.5 Hz, 3H), 1.04 (t, J=7.5 Hz, 6H), 1.36 (m, 4H), 1.48 (m, 4H), 1.67 (m, 2H), 1.75 (m, 4H), 2.68 (t, J=7.5 Hz, 2H), 3.60 (t, J=8.5 Hz, 4H), 6.86 (d, J=9.0 Hz, 2H), 7.33 (d, J=8.0 Hz, 2H), 7.38 (d, J=9.0 Hz, 2H), 7.53 (d, J=8.0 Hz, 2H) ppm. FT-IR (KBr): υ=2935, 2850, 2200, 1601, 1379, 1012, 816, 645, 559 cm^{-1}. MALDI-TOF-MS (dithranol): m/z: calc'd for $C_{39}H_{37}F_4N_5$: 651.30 g/mol, found: 652.4 g/mol $[MH]^+$. Elemental analysis calc'd (%) for $C_{39}H_{37}F_4N_5$ (651.30): C 71.87, H 5.72, N 10.75; found: C 71.89, H 5.71, N 10.74.

3. Results and discussion

*3.1. Synthesis of compounds **FTQ-1~FTQ-4***

The synthesis of donor-acceptor chromophores **FTQ-1** to **FTQ-4** was achieved through introducing amine-substituted aromatic precursors by high-yielding [2+2] cycloaddition-cycloreversion reactions using F_4-TCNQ as acceptor molecules. As shown in **Scheme 1**, all the acetylenic bonds reacted with the electron acceptor of F_4-TCNQ. The reaction of F_4-TCNQ could be fulfilled under ambient temperature, while enhancing the temperature to 100 °C allowed for more rapid completion of the reaction. Furthermore, one easy purification process was necessary because of the absence of byproducts, and yields were significantly high, ranging from 96% to 98%. The molecular structures of **FTQ** were confirmed by NMR, FT-IR, and MS spectra and elemental analysis. The **FTQ** dyes were stable

at ambient conditions and reasonably soluble in common organic solvents, such as DMSO, CH_2Cl_2, THF, acetone and acetonitrile (**Fig. S1**).

The cycloaddition-cycloreversion reaction of **b3** (~2×10^{-5} M) was initially investigated by UV/Vis/NIR spectroscopic titration experiments by adding acceptor molecule F_4-TCNQ to **b3** in chlorinated solvents (**Fig. 1a**). The absorption intensities of the precursor (**b3**) started to decrease, and two new charge transfer (CT) bands at 483 and 861 nm formed due to the presence of product **FTQ-3**. The peak positions of the CT bands remained unchanged, while the intensities linearly increased with the addition of F_4-TCNQ. Presence of one isosbestic point at 357 nm indicates there were no side reactions. The UV/Vis/NIR monitoring indicates that the electronic state of **FTQ-3** was modulated by F_4-TCNQ. Moreover, the two new CT bands of **FTQ-3** have almost perfect geometrical shapes (**Fig. 1b**). It is easy to separate the three peaks using software based on the Gaussian distribution, and the results are shown in **Fig. 1b**. Peaks A and B usually exhibit Gaussian distribution and the fitting curves meet the experimental curves very well. This suggests that each peak conceptually could represent one kind of chromophore. In accordance with the CT properties of every chromophore, the corresponding chemical structures were also inserted into **Fig. 1b**.

*3.2. PA effect of **FTQ-1~FTQ-4***

The PA intesnities of **FTQ** solutions with a concentration of 3×10^{-5} M were measured using MOST-128. As it is shown in **Fig. 2a**, the PA intensities of all the **FTQ** dyes were higher than that of ICG, which was used as the archetypal reference for dye-based PA contrast agents under the same experimental conditions. To give insight into the high PA intensities of **FTQs** and to cue the molecular design of NIR dyes for PAI, we measured the molar extinction coefficients (ε), and the thermal conversion efficiencies (η) according to the photothermal mechanism based equation of PA effect: $q \propto \Gamma \eta \mu_a F$ (1), where Γ is the Grueneisen parameter (dimensionless), μ_a is the optical absorption coefficient (cm^{-1}), η is the thermal conversion efficiency, and F is the local optical fluence ($J\cdot cm^{-2}$). [15] The major parameters for re-construction of the PA signals were the optical absorption coefficient (μ_a) and the thermal conversion efficiency (η).

Compounds **FTQ-1** through **FTQ-4** containing the same parent skeleton and different substitutions were used to measure the UV/Vis/NIR absorption spectra at a concentration of 3×10^{-5} M (**Fig. 2b**). The UV/Vis/NIR absorption spectra of **FTQ** were in accordance with the wavelength-dependent PA intensity diagrams (**Fig. 2b** and **c**), supporting the strong correlation between the NIR absorption and PA effect. The parent molecule **FTQ-1** showed the NIR absorption with the maxima at 817 nm and the molar extinction coefficient of 2.2×10^4 L mol^{-1} cm^{-1}. The compound **FTQ-3** showed almost the same absorption properties as **FTQ-1** (maxima at 816 nm, $\varepsilon = 2.1 \times 10^4$ L mol^{-1} cm^{-1}) with introduction of an alkyl chain. Interestingly, with the introduction of the electron-donating *N*,*N*-dibutyl group as an auxochrome to **FTQ-2**, the molar extinction coefficient was increased to 4.5×10^4 L mol^{-1} cm^{-1} and the absorption peak was hypsochromically shifted to 790 nm compared to the parent molecule **FTQ-1**. However, the placement of an electron-withdrawing aldehyde group in the chromophore bathochromically shifted the NIR absorption peak of **FTQ-4** to 831 nm compared to **FTQ-1,** and the molar extinction coefficient increased to 3.8×10^4 L mol^{-1} cm^{-1}. Based on the above experimental results, we can conclude that the alkyl chains had almost no influence on the NIR absorption (wavelength and intensity). Electron-withdrawing groups tended to bathochromically shift the absorption of the **FTQ** in the NIR range. On the contrary, electron-donating groups tended to

induce a hypsochromicshift of the absorption. Importantly, both the electron-donating and withdrawing groups resulted in increased absorption intensity with a hypsochromic shift. [16] Based on the large molar extinction coefficients (ε), **FTQ-2** and **FTQ-4** showed PA intensities 1.5×10^5 at 800 nm and 1.3×10^5 at 830 nm, respectively, which were higher than that of **FTQ-1** (9.9×10^4 at 820 nm) and **FTQ-3** (4.2×10^4 at 820 nm). The results are in accordance with the equation (1) based on the photothermal mechanism.

In addition, thermal conversion efficiencies (η) of **FTQ** dyes were also determined in order to evaluate their contributions to the resultant PA effects. The **FTQ** solutions with a concentration of 3×10^{-5} M were used to measure the thermal conversion efficiency. A 100 μL solution of **FTQ** was irradiated under the laser (400 mW) at the wavelength of maximum absorption for each **FTQ**. The temperatures were recorded by the thermal imaging system and the time-dependent temperature variation curves of **FTQ** are shown in **Fig. 2d**. The thermal conversion efficiencies (η) of the **FTQs** were calculated by fitting the curves of time-dependent temperature variations (**Fig. S2**). [17] **FTQ-2** and **FTQ-3** displayed high thermal conversion efficiencies of 51.5% and 53.9%, respectively (**Table 1**). Comparing these with the relatively low thermal conversion efficiencies of **FTQ-1** (η = 30.0%) and **FTQ-4** (η = 33.9%), it is proposed that the alkyl chains in **FTQ-2** and **FTQ-3** may contribute to the higher thermal conversion efficiencies due to the thermal vibration of the alkyl chains, since they have similar molecular structures. [18] **FTQ-3**, with the highest η value (53.9%), showed the lowest PA intensity (4.2×10^4 at 820 nm). This result was not supported by the photothermal equation (1), where the PA effect is directly related to the thermal conversion efficiency. For the series of **FTQ** NIR dyes, the photoacoustic waves may be also related to the electrostriction of the solvent, induced by charge transfer of the **FTQ** molecules. [19-21] The molecular simulation and quantum chemistry calculations were carried out for explanation (**Table 1** and details see SI). The possible conformational changes under photoirradiation may contribute to the PA effect for the series of **FTQs** aside from the photothermal mechanism, and make the **FTQ** dyes show higher PA intensities when compared to ICG. [22]

3.3. PA imaging in vitro

To demonstrate the potential application of the **FTQs** in PAI, we loaded **FTQ-4** into a well-defined hydrophobic bilayer of liposomes, which have been widely applied as drug delivery vehicles. [23] Briefly, L-α-phosphatidylcholine and cholesterol (4:1 w:w) were dissolved in an ethanol solution. Afterward, the **FTQ-4**-containing DMSO solution was added into the aforementioned premixed ethanol solution. The resulting mixture was subsequently injected into phosphate-buffered saline (PBS) and stirred for 1 h. The **FTQ-4** molecules were preferentially embedded into a hydrophobic phospholipid bilayer of liposome through hydrophobic interactions. [24] The morphology of **FTQ-4** ⊂ L in PBS (pH=7.4) was investigated by transmission electron microscopy (TEM). Under the mass ratio (1:10) of **FTQ-4** and phospholipids, uniform vesicular structures of **FTQ-4** ⊂ L with a size of 42 ± 18 nm were observed (**Fig. 3b**). The technique of dynamic light scattering (DLS) measured a hydrodynamic diameter of **FTQ-4** ⊂ L of 79 ± 12 nm with narrow size distribution (**Fig. S4**). The **FTQ-4** ⊂ L with a 1:10 mass ratio displayed almost the same absorption (λ_{max} = 815 nm) with that of **FTQ-4** in DMSO, indicating **FTQ-4** was successfully loaded into the liposome (**Fig. 3a**). Furthermore, the **FTQ-4** ⊂ L was utilized as a contrast agent for PA imaging *in vitro* by using human breast cancer MCF-7 cells as a model cell line. The MCF-7 cells grown on a Petri dish (~10^7 cells) were incubated with **FTQ-4** ⊂ L (10 μM based on **FTQ-4** molecules) and ICG (10 μM) separately for 2 h at 37

°C. The treated cells in PBS were mixed with a 2% ultrapure agarose solution (V_1/V_2 = 1:1), and then added into the wells of an agarose gel phantom made in advance. PA imaging was collected using Multi-Spectral Optoacoustic Tomography (MSOT) under an 815 nm laser excitation at different time intervals. The PA signals of **FTQ-4** ⊂ L in the cells were recorded in an agarose gel for PAI. About 50% of the PA signals could be maintained in **FTQ-4** ⊂ L treated cells for 96 h. As a reference, it only took 12 h for PA signals of ICG treated cells to decrease by half (**Fig. 3c**). These results indicate that **FTQ-4** could be used as a contrast agent for PAI when doping into the nano-sized liposomes. In addition, the cytotoxicity of **FTQ-4** ⊂ L nanovesicles was evaluated through CCK-8 assays to determine the metabolic viability of MCF-7 cells.[25] No significant cytotoxicity was observed with a concentration up to 10 μM under our experimental conditions (**Fig. S5**).

4. Conclusions

In summary, we have prepared a series of NIR absorbing dyes through a cycloaddition-cycloreversion reaction. The systematic investigation of the NIR dyes indicates that substitutions with electron-donating or electron-withdrawing groups can enhance the molar extinction coefficients and PA intensities. Finally, the NIR absorbing dyes with good stability and high PA intensities were utilized to image cells in an agarose gel for an extended period of time by loading them into nano-sized liposomes. Our results systematically illuminate the influences on PA effects and provide guidance for the design of NIR absorbing dyes for high-performance PA bioimaging. The investigation into water-soluble NIR absorbing dyes with high PA intensities is in progress in our lab.

Acknowledgements

This work was supported by National Natural Science Foundation of China (51473188, 21374026, 21304023, and 51303036), National Basic Research Program of China (973 Program, 2013CB932701), Beijing Natural Science Foundation (2132053) and the 100-Talent Program of the Chinese Academy of Science (Y2462911ZX).

Appendix A. Supplementary data

Supplementary data related to this article can be found at http://dx.doi.org/XXX

References

[1] Xu M, Wang LV. Photoacoustic imaging in biomedicine. Rev Sci Instrum 2006;77:041101-1--22.

[2] Zhang J, Qiao Z, Yang P, Pan J, Wang L, Wang H. Recent advances in near-infrared absorption nanomaterials as photoacoustic contrast agents for biomedical imaging. Chin J Chem 2015;33:35-52.

[3] Cheng K, Kothapalli SR, Liu H, Koh AL, Jokerst JV, Jiang H, et al. Construction and validation of nano gold tripods for molecular imaging of living subjects. J Am Chem Soc 2014;136:3560-71.

[4] De La Zerda A, Zavaleta C, Keren S, Vaithilingam S, Bodapati S, Liu Z, et al. Carbon nanotubes as photoacoustic molecular imaging agents in living mice. Nat Nanotechnol 2008;3:557-62.

[5] Kim J-W, Galanzha EI, Shashkov EV, Moon H-M, Zharov VP. Golden carbon nanotubes as multimodal photoacoustic and photothermal high-contrast molecular agents. Nat Nanotechnol 2009;4:688-94.

[6] Pu K, Shuhendler AJ, Jokerst JV, Mei J, Gambhir SS, Bao Z, et al. Semiconducting polymer nanoparticles as photoacoustic molecular imaging probes in living mice. Nat Nanotechnol 2014;9:233-9.

[7] Lovell JF, Jin CS, Huynh E, Jin H, Kim C, Rubinstein JL, et al. Porphysome nanovesicles generated by porphyrin bilayers for use as multimodal biophotonic contrast agents. Nat Mater 2011;10:324-32.

[8] Akers WJ, Kim C, Berezin M, Guo K, Fuhrhop R, Lanza GM, et al. Noninvasive photoacoustic and fluorescence sentinel lymph node identification using dye-loaded perfluorocarbon nanoparticles. ACS Nano 2011;5:173-82.

[9] Wang LV, Hu S. Photoacoustic tomography: in vivo imaging from organelles to organs. Science 2012;335:1458-62.

[10] Ntziachristos V, Razansky D. Molecular imaging by means of multispectral optoacoustic tomography (MSOT). Chem Rev 2010;110:2783-94.

[11] Ntziachristos V. Going deeper than microscopy: the optical imaging frontier in biology. Nat Methods 2010;7:603-14.

[12] Wang D, Wang X, Zhao Y, Gao H, Xing Y, Yang H. Ladder-type poly(benzopentalene) derivatives with tunable energy levels by "click" reaction. Poly Chem 2012;3:914-9.

[13] Wang D, Michinobu T, One-step synthesis of ladder-type fused poly(benzopentalene) derivatives with tunable energy levels by variable substituents. J. Polym. Sci., Part A: Polym. Chem. 2011;49:72-81.

[14] Zhang W-S, Wang D, Cao H, Yang H. Energy level tunable pre-click functionalization of [60]fullerene for nonlinear optics. Tetrahedron 2014;70:573-7.

[15] Danielli A, Favazza CP, Maslov K, Wang LV. Picosecond absorption relaxation measured with nanosecond laser photoacoustics. Appl Phys Lett 2010;97:163701.

[16] McHale JL. Molecular spectroscopy. 1st ed: Prentice Hall; 1998.

[17] Zeng J, Goldfeld D, Xia Y. A Plasmon-assisted optofluidic (PAOF) system for measuring the photothermal conversion efficiencies of gold nanostructures and controlling an electrical switch. Angew Chem Int Ed 2013;52:4169-73.

[18] Chen HL, Huang YF, Lim TS, Su CH, Chen PH, Su AC, et al. Excited-state backbone twisting of polyfluorene as detected from photothermal after-effects. J Phys Chem B 2009;113:8527-31.

[19] Braslavsky SE, Heibel GE. Time-resolved photothermal and photoacoustic methods applied to photoinduced processes in solution. Chem Rev 1992;92:1381-410.

[20] Feitelson J, Mauzerall D. Photoacoustic evaluation of volume and entropy changes in energy and electron transfer. triplet state porphyrin with oxygen and naphthoquinone-2-sulfonate. J Phys Chem 1996;100:7698-703.

[21] Frenette M, Hatamimoslehabadi M, Bellinger-Buckley S, Laoui S, La J, Bag S, et al. Shining light on the dark side of imaging: excited state absorption enhancement of a bis-styryl BODIPY photoacoustic contrast agent. J Am Chem Soc 2014;136:15853-6.

[22] Espinosa E, Molins E, Lecomte C. Hydrogen bond strengths revealed by topological analyses of experimentally observed electron densities. Chem Phys Lett 1998;285:170-3.

[23] Fan K, Cao C, Pan Y, Lu D, Yang D, Feng J, et al. Magnetoferritin nanoparticles for targeting and visualizing tumour tissues. Nat Nanotechnol 2012;7:459-64.

[24] Zhang D, Zhao Y-X, Qiao Z-Y, Mayerhöffer U, Spenst P, Li X-J, et al. Nano-confined squaraine dye assemblies: new photoacoustic and near-infrared fluorescence dual-modular imaging probes in vivo. Bioconjug Chem 2014;25:2021-9.

[25] Takeuchi A, Mishina Y, Miyaishi O, Kojima, E, Hasegawa T, Isobe K. Heterozygosity with respect to Zfp148 causes complete loss of fetal germ cells during mouse embryogenesis. Nat Genet 2003;33:172-6.

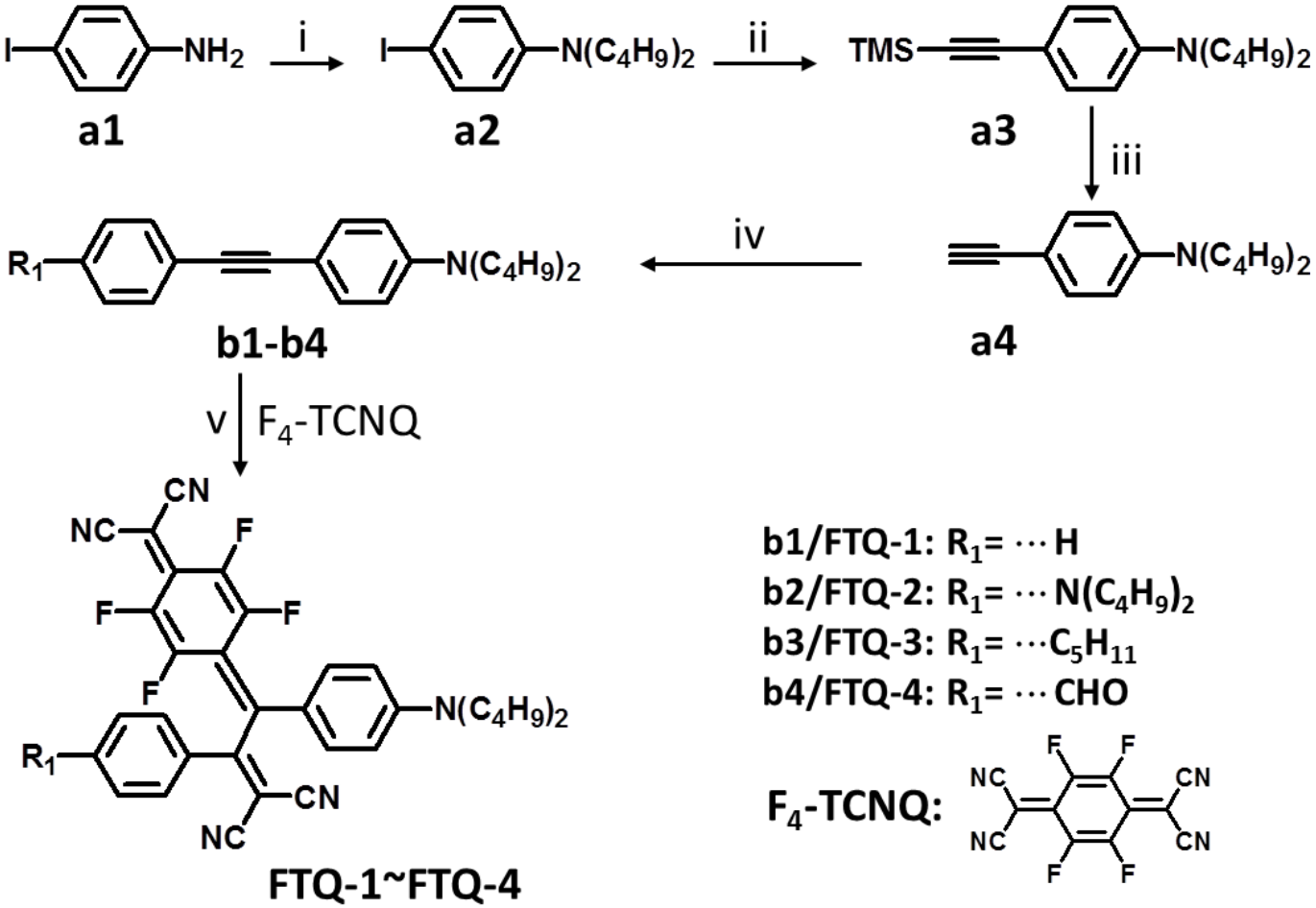

Scheme 1. Molecular structures of compounds **a**, **b** and **FTQ** and their synthetic routes: (i) C_4H_9I, K_2CO_3, DMF, 100 °C, 12 h. (ii) Ethynyltrimethylsilane, TEA/THF, $Pd(PPh_3)_2Cl_2$, CuI, 40 °C, 12 h. (iii) K_2CO_3, CH_3OH/THF. (iv) 4-Bromophenyl-R_1, TEA/THF, $Pd(PPh_3)_2Cl_2$, CuI, 80 °C, 12 h. (v) F_4-TCNQ, chlorobenzene, 100 °C, 2 h.

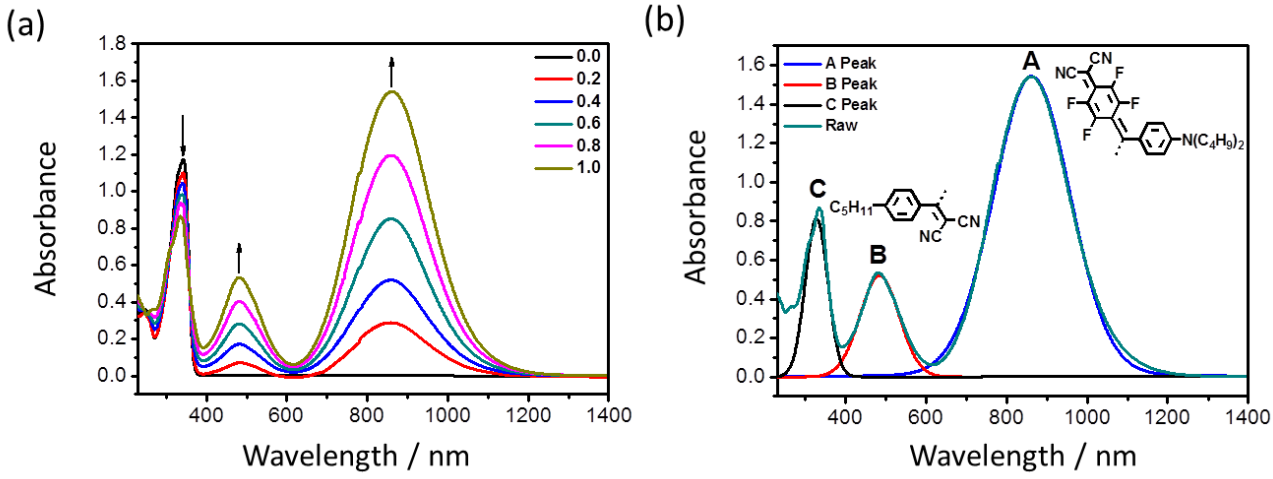

Fig. 1. (a) UV/Vis/NIR spectral changes of **b3** (~2×10^{-5} M) upon titration with F_4-TCNQ (0-1.0 equiv.) in chlorinated solvent at 100 °C. (b) The **FTQ-3** UV/Vis/NIR was fitted based on based on the Gaussian distribution, A Peak in blue, B peak in red and C peak in dark green.

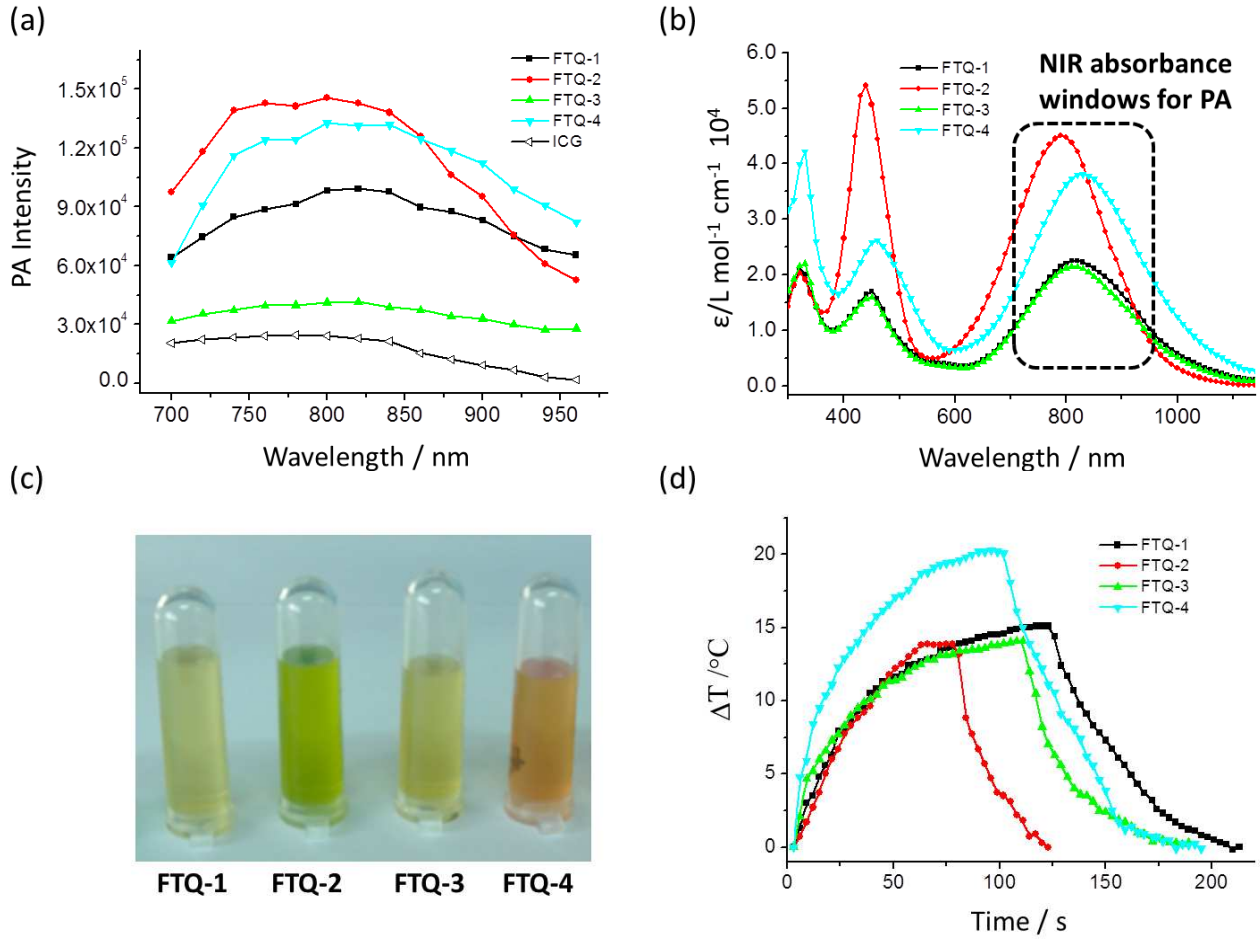

Fig. 2. (a) The PA intensities of **FTQ** and ICG measured in DMSO (3×10^{-5} M). (b) The UV/Vis/NIR spectra of the NIR dyes **FTQ** and (c) corresponding photos of **FTQ** solutions taken by digital camera. (d) The heating/cooling curves of **FTQ** at different times. The energy input from lasers was 400 mW at about 800 nm with an irradiated diameter of 2 mm.

Table 1. The summary of PA intensity, thermal conversion efficiency (η), molar extinction coefficient (ε), and corresponding sum of main intramoleular interaction energy (V(r)) in both states of FTQ molecules.

FTQ	PA (10^4)	ε (10^4, L/mol/cm)	η (%)	V(r) (KJ/mol)	
				S1	S2
1	9.9	2.2	30.0	-90.485	-78.611
2	14.6	4.5	51.5	-107.156	-105.537
3	4.2	2.1	53.9	-89.996	-78.716
4	13.2	3.8	33.9	-90.073	-78.223

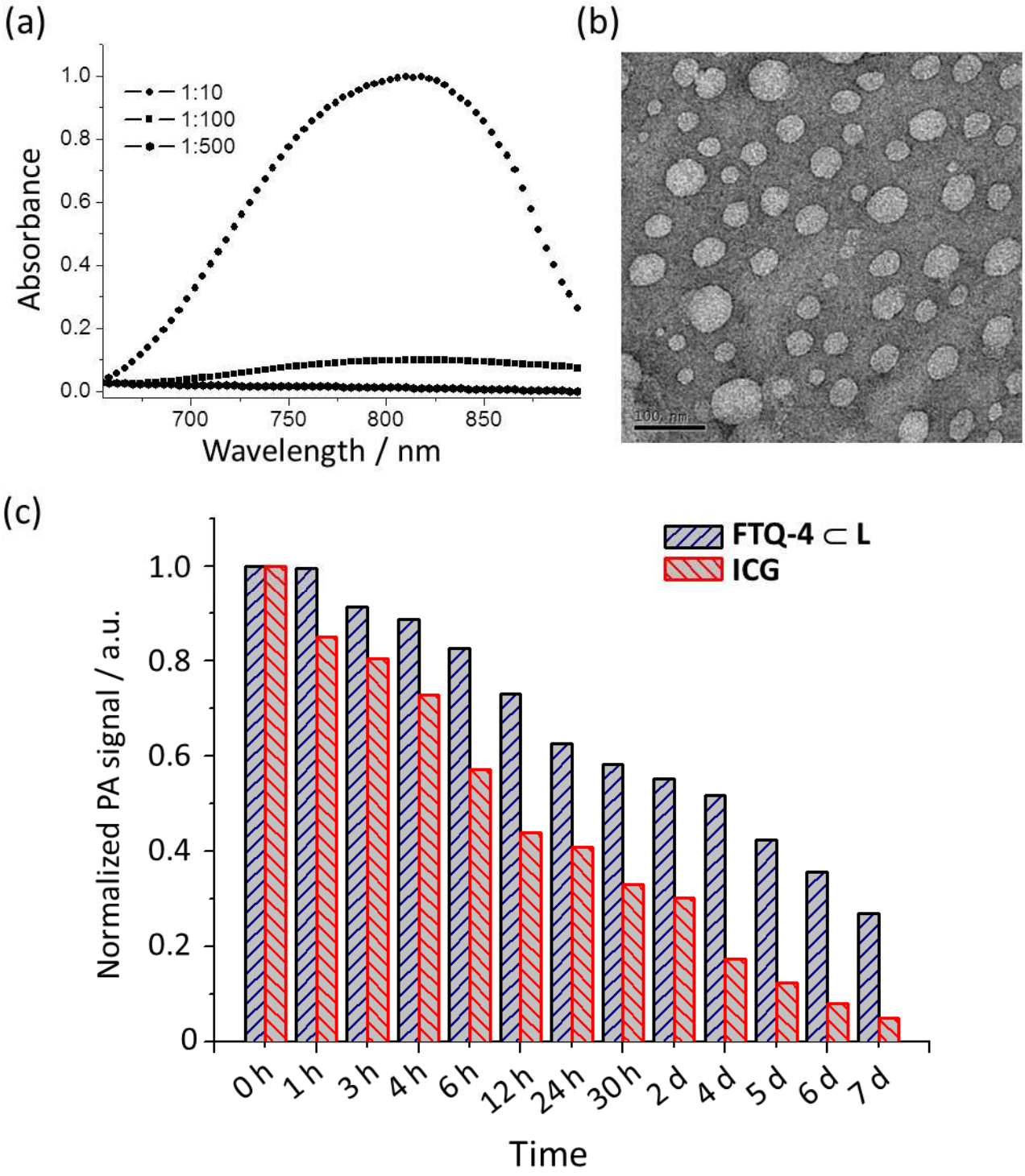

Fig. 3. UV/Vis/NIR absorption spectra of **FTQ-4** ⊂ L with different ratios of **FTQ-4** to liposome in PBS. (b) TEM images of **FTQ-4** ⊂ L. (c) PA imaging of **FTQ-4** ⊂ L incubated in cells, which was added to agarose gel wells and embedded into the agarose gel phantom. The phantom was imaged using MOST 128 with an 815 nm excitation pulse laser at different time intervals.

- A new class of dyes with NIR absorption was designed and prepared.
- The NIR dyes showed excellent photoacoustic effect.
- Charge transfer of NIR dyes may contribute to photoacoustic effect.